



Published in final edited form as:

J Vasc Interv Radiol. 2015 July ; 26(7): 1052–1058. doi:10.1016/j.jvir.2015.01.016.

Pleural Puncture that Excludes the Ablation Zone Decreases the Risk of Pneumothorax after Percutaneous Microwave Ablation in Porcine Lung

Kyungmouk Steve Lee, MD, Haruyuki Takaki, MD, PhD, Hooman Yarmohammadi, MD, Govindarajan Srimathveeravalli, PhD, Kerith Luchins, DVM, Sébastien Monette, DMV, MVSc, Sreejit Nair, MD, Sirish Kishore, MD, and Joseph P. Erinjeri, MD, PhD

Department of Radiology (K.S.L., H.T., H.Y., G.S., S.N., S.K., J.P.E), Research Animal Resource Center Memorial (K.L.), and Laboratory of Comparative Pathology (S.M.), Memorial Sloan-Kettering Cancer Center, 1275 York Avenue, H-118, New York, NY 10065

Abstract

Purpose—To test the hypothesis that the geometry of probe placement with respect to the pleural puncture site affects the risk of pneumothorax after microwave (MW) ablation in the lung.

Materials and Methods—Computed tomography–guided MW ablation of the lung was performed in 8 swine under general anesthesia and mechanical ventilation. The orientation of the 17-gauge probe was either perpendicular (90°) or parallel (< 30°) with respect to the pleural puncture site, and the ablation power was 30 W or 65 W for 5 minutes. After MW ablation, swine were euthanized, and histopathologic changes were assessed. Frequency and factors affecting pneumothorax were evaluated by multivariate analysis.

Results—Among 62 lung MW ablations, 13 (21%) pneumothoraces occurred. No statistically significant difference was noted in the rate of pneumothorax between the perpendicular and the parallel orientations of the probe (31% vs 14%; odds ratio [OR], 2.8; $P = .11$). The pneumothorax rate was equal for 65-W and 30-W ablation powers (21% and 21%; OR, 1.0; $P = .94$). Under multivariate analysis, 2 factors were independent positive predictors of pneumothorax: ablation zone inclusive of pleural insertion point (OR, 7.7; $P = .02$) and time since intubation (hours) (OR, 2.7; $P = .02$).

Conclusions—Geometries where the pleural puncture site excluded the ablation zone decreased pneumothorax in swine undergoing MW ablation in the lung. Treatment planning to ensure that the pleural puncture site excludes the subsequent ablation zone may reduce the rate of pneumothorax in patients undergoing MW ablation in the lung.

The most common complication after percutaneous thermal ablation in the lung is pneumothorax. Pneumothorax may occur in 11%–63% of patients; a few of these patients require chest tube placement that may result in prolonged hospitalization (1–7). In radiofrequency (RF) ablation of pulmonary tumors, risk factors for pneumo-thorax include

Address correspondence to J.P.E.; erinjerj@mskcc.org.

None of the authors have identified a conflict of interest.

emphysema, small tumor size, absence of prior pulmonary surgery, and traversal of major fissure by the probe (1–5). Prior studies of RF ablation showed that contact of the ablation zone with the pleura can lead to delayed or recurrent pneumothorax and that tract ablation should be avoided (8,9). Microwave (MW) ablation can be used at much higher energy than RF ablation and results in larger tumor ablation volumes, higher intratumoral temperatures, and less susceptibility to heat sink effect (10,11). However, there have been reports of intractable pneumothorax and the formation of bronchopleural fistula after MW ablation in the lung (12,13). It is unknown how the MW energy deposition directly on the pleura affects the risk of pneumothorax. The purpose of this study was to test the hypothesis that the geometry of probe placement with respect to the pleural puncture site affects the risk of pneumothorax after percutaneous computed tomography (CT)-guided MW ablation in a porcine lung model.

MATERIALS AND METHODS

Animals

All experiments were performed with approval from the Institutional Animal Care and Use Committee of our institution and in accordance with the Guide for Care and Use of Laboratory Animals issued by the National Research Council. Eight swine (Yorkshire female) weighing 35–45 kg were used in this study.

Experimental Setup

The swine received sedation (tiletamine/zolazepam and xylazine), anesthesia (isoflurane), and preemptive analgesics (buprenorphine and carprofen). After endotracheal intubation, mechanical ventilation was initiated without positive end expiratory pressure (ventilatory pressure, 18–22 cm H₂O; tidal volume, 5–10 mL/kg). Under CT guidance (LightSpeed 16; GE Healthcare, Milwaukee, Wisconsin), a 17-gauge MW ablation probe (Certus 140 PR 15 Probe; NeuWave Medical, Madison, Wisconsin) was percutaneously inserted into the porcine lung by a single operator in either the perpendicular or the parallel orientation. The needle orientation was defined as “perpendicular” if the angle between the needle and the pleural puncture site was 90° (Fig. a). The needle orientation was defined as “parallel” if the angle between the needle and the pleural puncture site was < 30° (Fig. d). For each ablation, a single pleural puncture was made during the insertion of the MW probe. If there was any adjustment of the probe position with respect to the pleura, the pleural puncture site remained constant, and only minor angle changes were made. The tip of the ablation probe did not violate any lung fissures, and all ablations were performed away from any major bronchus. There was no violation of the instructions for use of the MW ablation device.

Randomization was performed with regard to probe orientation and lung laterality during MW ablation. The first lung to be ablated was randomized—in four swine, the right lung was ablated first; in four swine, the left lung was ablated first. The probe orientation was also randomized—in four swine, the perpendicular orientation was used as the initial ablative approach; in four swine, the parallel orientation was used as the initial approach. For the first four swine, MW ablations were performed for 5 minutes at 30 W; for the second four swine, ablations were performed for 5 minutes at 65 W. During each ablation, the

maximum temperature of the probe was recorded. Immediately after each ablation, CT images were acquired to evaluate the size of the ablation zone. CT images of the entire chest were obtained immediately after and 5 minutes after ablation to identify any pneumothorax. When a pneumothorax occurred, an 8-F chest tube was placed percutaneously into the thorax under CT guidance. The chest tube was connected to a drainage system and placed onto continuous low wall suction. If a pneumothorax developed in one lung, no further ablations were performed in that lung, and the contralateral lung was used for subsequent ablations. The animals were euthanized with an overdose of pentobarbital after the procedure.

Measurements

Based on the CT images, the following measurements were obtained: dimensions of the ablation zone (long axis and short axis), distance from the emitting point of the MW probe to the pleural puncture site (the emitting point was 1 cm from the tip of the probe), distance from the emitting point to the nearest adjacent pleura, length of pleural contact with the ablation zone, and whether or not the ablation zone includes the pleural puncture site. The time elapsed since endotracheal intubation was recorded. The number of ablations performed in each lung was also documented.

Histopathologic Examination

At the conclusion of the MW ablation session, the swine was euthanized using intravenous injections of pento-barbital and phenytoin. Subsequently, gross dissection was performed, and lungs were removed en bloc. Gross photographs of the ablated lung and pleura were obtained. The ablation zone and surrounding pleura were harvested from the lungs, fixed by immersion in 10% neutral buffered formalin, routinely processed for histology, embedded in paraffin, sectioned at 4- μ m thickness, and stained with hematoxylin and eosin.

Statistical Analysis

To determine the factors predicting pneumothorax after MW ablation, univariate logistic regression was performed for both categorical variables (perpendicular or parallel geometry, ablation zone includes pleural puncture site yes/no, presence of pneumothorax) and continuous variables. The factors significant in the univariate model underwent a multivariate logistic regression. *P* values < .05 were considered statistically significant. Statistical analysis was performed using SAS software version 9.4 (SAS Institute, Cary, North Carolina).

RESULTS

There were 62 percutaneous CT-guided MW ablations performed in the porcine lung (Table 1). The ablations were performed for 5 minutes at 30 W in 34 (55%) of the cases and at 65 W in 28 (45%). In 36 (58%) ablations, the probe was in a parallel orientation with respect to the pleura, and in 26 (42%) ablations, the probe was perpendicular to the pleura. The mean distance between the pleural puncture site and the emitting point of the MW ablation probe was 2.4 cm \pm 1.2. The mean distance between the emitting point of the probe and the nearest

adjacent pleura was $1.2 \text{ cm} \pm 0.4$. The ablation zone included the pleural puncture site in 32 (52%) of the cases and did not include the pleural puncture site in 30 (48%) ablations.

Pneumothorax occurred in 13 of 62 (21%) MW ablations (Table 2). No statistically significant difference was noted in the rate of pneumothorax between the two different orientations of the probes, although more pneumothoraces did occur with the perpendicular approach versus the parallel approach (31% vs 14%; odds ratio [OR], 2.8; $P = .11$). The pneumothorax rate was equal for both ablation powers, 65 W and 30 W (21% and 21%; OR, 1.0; $P = .94$). The maximum probe temperature did not differ between the ablations with pneumothorax and the ablations without pneumothorax ($93^\circ\text{C} \pm 15$ and $91^\circ\text{C} \pm 17$; OR, 1.0; $P = .66$).

Under univariate analysis, there were three factors that were significantly associated with pneumothorax after MW ablation (Table 3): ablation zone includes pleural puncture site (OR, 4.1; $P = .049$), number of ablations in each lung (OR, 1.5; $P = .04$), and time since intubation (h) (OR, 2.8; $P = .01$). Other factors that did not reach significance in predicting pneumothorax included distance between emitting point to pleural puncture (cm) (OR, 0.6; $P = .14$), distance between emitting point to closest pleura (cm) (OR, 0.5; $P = .42$), ablation zone long axis (cm) (OR, 0.6; $P = .33$), ablation zone short axis (cm) (OR, 0.4; $P = .21$), ablation zone area (cm^2) (OR, 0.8; $P = .18$), and pleural contact with ablation zone (cm) (OR, 0.9; $P = .74$). Under multivariate analysis, two of the three significant univariate factors remained independent positive predictors of pneumothorax after MW ablation: ablation zone inclusive of pleural insertion point (OR, 7.7; $P = .02$) and time since intubation (h) (OR, 2.7; $P = .02$) (Table 4).

Histopathologic Results

When the ablation zone included the pleural puncture site, there was disruption of the full thickness of the pleura (connective tissue and monolayer of mesothelial cells) (Fig, c, i). The ablation zones were characterized by a central area displaying basophilic discoloration and hyalinization of collagen (thermal effect), mild cellular cytoplasmic hypereosinophilia and nuclear shrinkage (early morphologic evidence of cell death), and alveolar edema. When the ablation zone was exclusive of the pleural puncture site, the pleura remained intact with a rim of vascular hyperemia associated with the periphery of the ablation zone (Fig, f).

DISCUSSION

The results of this study show that the two factors associated with the occurrence of pneumothorax after MW ablation in porcine lung were (*i*) the ablation zone included the pleural puncture site and (*ii*) time elapsed since endotracheal intubation. Although the pneumo-thorax rate for the perpendicular probe orientation was higher than the pneumothorax rate for the parallel approach, this difference was not statistically significant. Even for the parallel approach, there was an increased risk of pneumothorax if the ablation zone included the site of pleural puncture. The results of this swine study indicate that to minimize the risk of pneumothorax it is prudent to avoid overlapping the ablation zone with the pleural puncture site. If general anesthesia is used during MW ablation in a patient,

minimizing the time elapsed since endotracheal intubation may result in less air entry into ablation-related pleural defects and reduce the risk of pneumothorax.

This study of MW ablation is consistent with a prior study of RF ablation in which Yoshimatsu et al (9) concluded that the contact of the ground-glass opacity that emerged around the ablated lesion with the pleura significantly correlated with the occurrence of delayed or recurrent pneumothorax. Clasen et al (8) reported that tract ablation during pulmonary RF ablation may contribute to bronchopleural fistula and hypothesized that coagulation of the visceral pleura and adjacent lung tissue induces dehydration and reduces the elastic properties of the lung tissue to seal the puncture. However, there is also contradictory literature from Tajiri et al (14), who found that higher pleural temperature appeared to be associated with pleural effusion but not pneumothorax.

The visceral pleura comprises a single layer of meso-thelial cells and a thick layer of connective tissue (composed primarily of collagen) (15). When the ablation zone includes the pleural puncture site, there is dual disturbance of the pleura in the form of thermal injury from MW energy and mechanical trauma from the probe. Similarly, there is mechanical and thermal injury to the surrounding alveoli resulting in alveolar rupture. When these injuries lead to communication of the alveoli (or airway) with the intrapleural space, air flows from the alveoli into the intrapleural space until the pressure difference is eliminated. There is resultant accumulation of air in the intrapleural space (ie, a pneumothorax, or rarely a bronchopleural fistula) (16). Histologic analysis of the ablated lung in this swine study demonstrated evidence of pleural injury and thermal ablation that disrupted the pleural collagen and mesothelium, causing a rent in the visceral pleura that can communicate with a ruptured alveolus to yield an iatrogenic pneumothorax (17,18). The findings in this swine study are consistent with prior studies in rabbit lung models using RF ablation (19). In the study by Okuma et al (19), histologic examination showed pleural sloughing at the point of needle insertion and ring-shaped thermal injury in the chest wall similar to the histology seen in the evidence of pleural thermal injury after RF ablation of lung tissues adjacent to the pleura (14).

Time elapsed since intubation was the most significant factor associated with the development of pneumothorax after MW ablation in this swine study. Mechanical ventilation is known to induce barotrauma with an incidence of 4%–15% (20,21). Ventilator-associated pneumothorax is related to rupturing of the alveoli with dissection of air into the intrapleural space. In animal studies, there is evidence that transalveolar pressure and alveolar overdistention, rather than high airway pressure, are the primary causes of barotrauma and ventilator-induced lung injury (21,22). Pneumothorax is unusual in intubated patients with normal lungs, and most patients with pneumothorax related to mechanical ventilation have underlying pulmonary disease, most often acute respiratory distress syndrome in which the lung is physiologically small with low compliance (20). Thermal ablation induces an acute injury to the lung that may mimic acute pulmonary pathology; combining thermal ablation and mechanical ventilation likely has a multiplicative effect on the risk of pneumothorax. Although no positive end expiratory pressure was used in this experiment, mechanical ventilation increases the flow of gas through a pleural defect after ablation, and there may be a more rapid increase in intrapleural pressure with earlier

progression to pneumothorax (23). Longer time on mechanical ventilation may allow for greater volume of gas to enter the ablation-related pleural defect, resulting in an increased occurrence of pneumothorax.

This study has limitations. The porcine lungs used in this experiment were normal without evidence of emphysema or malignancy. Emphysema and small tumor size are known risk factors for pneumothorax after thermal ablation (2–4). In this study, multiple ablations were performed in each lung, and the pneumothorax may be the result of cumulative effect of the ablations and not attributable to a single ablation performed in a particular manner. The sample size of this study was small with only 62 MW ablations in eight swine, and certain parameters known to be risk factors in prior studies, such as aerated lung traversed by probe, may not have reached statistical significance. Another limitation was that the observer was not blinded to the therapy when the pneumothorax was assessed because a chest tube needed to be placed immediately after a pneumothorax occurred. Only MW ablation was studied, and the results of this experiment may not be applicable to other forms of ablation including cryoablation and RF ablation. All experiments in this large animal study were done under general anesthesia using mechanical ventilation, which is not always the case in clinical practice, in which many thermal ablations are performed using only moderate conscious sedation. Lastly, delayed or recurrent pneumothorax after thermal ablation is not rare and occurs at a mean duration of 24 hours after ablation (22,23); this issue could not be addressed because this experiment was a nonsurvival study. Despite these limitations, this experimental study identified two factors that should be considered to perform MW ablation in the lung safely.

In conclusion, geometries where the pleural puncture site excluded the ablation zone decreased pneumothorax in swine undergoing MW ablation in the lung. Treatment planning to ensure that the pleural puncture site excludes the subsequent ablation zone may reduce the rate of pneumothorax in patients undergoing MW ablation in the lung.

Acknowledgments

This study was funded by the 2013 Society of Interventional Radiology Foundation Radiology Resident Research Grant to K.S.L.

ABBREVIATIONS

MW	microwave
OR	odds ratio

References

1. Kashima M, Yamakado K, Takaki H, et al. Complications after 1000 lung radiofrequency ablation sessions in 420 patients: a single center's experiences. *AJR Am J Roentgenol*. 2011; 197:W576–W580. [PubMed: 21940529]
2. Hiraki T, Tajiri N, Mimura H, et al. Pneumothorax, pleural effusion, and chest tube placement after radiofrequency ablation of lung tumors: incidence and risk factors. *Radiology*. 2006; 241:275–283. [PubMed: 16908680]

3. Yamagami T, Kato T, Hirota T, Yoshimatsu R, Matsumoto T, Nishimura T. Pneumothorax as a complication of percutaneous radio-frequency ablation for lung neoplasms. *J Vasc Interv Radiol*. 2006; 17:1625–1629. [PubMed: 17057004]
4. Okuma T, Matsuoka T, Yamamoto A, et al. Frequency and risk factors of various complications after computed tomography-guided radiofrequency ablation of lung tumors. *Cardiovasc Intervent Radiol*. 2008; 31:122–130. [PubMed: 17985181]
5. Nour-Eldin N-EA, Naguib NNN, Saeed A-S, et al. Risk factors involved in the development of pneumothorax during radiofrequency ablation of lung neoplasms. *AJR Am J Roentgenol*. 2009; 193:W43–W48. [PubMed: 19542382]
6. Zheng A, Wang X, Yang X, et al. Major complications after lung microwave ablation: a single-center experience on 204 sessions. *Ann Thorac Surg*. 2014; 98:243–248. [PubMed: 24793688]
7. Liu H, Steinke K. High-powered percutaneous microwave ablation of stage I medically inoperable non-small cell lung cancer: a preliminary study. *J Med Imaging Radiat Oncol*. 2013; 57:466–474. [PubMed: 23870347]
8. Clasen S, Kettenbach J, Kosan B, et al. Delayed development of pneumothorax after pulmonary radiofrequency ablation. *Cardiovasc Intervent Radiol*. 2009; 32:484–490.
9. Yoshimatsu R, Yamagami T, Terayama K, Matsumoto T, Miura H, Nishimura T. Delayed and recurrent pneumothorax after radiofrequency ablation of lung tumors. *Chest*. 2009; 135:1002–1009. [PubMed: 19017870]
10. Brace CL, Hinshaw JL, Laeseke PF, Sampson LA, Lee FTJ. Pulmonary thermal ablation: comparison of radiofrequency and microwave devices by using gross pathologic and CT findings in a swine model. *Radiology*. 2009; 251:705–711. [PubMed: 19336667]
11. Crocetti L, Bozzi E, Faviana P, et al. Thermal ablation of lung tissue: in vivo experimental comparison of microwave and radiofrequency. *Cardiovasc Intervent Radiol*. 2010; 33:818–827. [PubMed: 20442998]
12. Bui JT, Gaba RC, Knuttinen MG, et al. Microwave lung ablation complicated by bronchocutaneous fistula: case report and literature review. *Semin Intervent Radiol*. 2011; 28:152–155. [PubMed: 22654252]
13. Alexander ES, Healey TT, Martin DW, Dupuy DE. Use of endobronchial valves for the treatment of bronchopleural fistulas after thermal ablation of lung neoplasms. *J Vasc Interv Radiol*. 2012; 23:1236–1240. [PubMed: 22920983]
14. Tajiri N, Hiraki T, Mimura H, et al. Measurement of pleural temperature during radiofrequency ablation of lung tumors to investigate its relationship to occurrence of pneumothorax or pleural effusion. *Cardiovasc Intervent Radiol*. 2008; 31:581–586. [PubMed: 18197451]
15. Jantz MA, Antony VB. Pathophysiology of the pleura. *Respiration*. 2008; 75:121–133. [PubMed: 18332619]
16. Baumann MH, Noppen M. Pneumothorax. *Respirology*. 2004; 9:157–164. [PubMed: 15182264]
17. Barton ED, Rhee P, Hutton KC, Rosen P. The pathophysiology of tension pneumothorax in ventilated swine. *J Emerg Med*. 1997; 15:147–153. [PubMed: 9144053]
18. Sharma A, Jindal P. Principles of diagnosis and management of traumatic pneumothorax. *J Emerg Trauma Shock*. 2008; 1:34–41. [PubMed: 19561940]
19. Okuma T, Matsuoka T, Yamamoto A, et al. Chest wall temperature during radiofrequency ablation in a normal rabbit lung model. *Jpn J Radiol*. 2010; 28:48–52. [PubMed: 20112093]
20. Hsu C-W, Sun S-F. Iatrogenic pneumothorax related to mechanical ventilation. *World J Crit Care Med*. 2014; 3:8–14. [PubMed: 24834397]
21. Gammon RB, Shin MS, Buchalter SE. Pulmonary barotrauma in mechanical ventilation. Patterns and risk factors. *Chest*. 1992; 102:568–572. [PubMed: 1643949]
22. Dreyfuss D, Saumon G. Ventilator-induced lung injury: lessons from experimental studies. *Am J Respir Crit Care Med*. 1998; 157:294–323. [PubMed: 9445314]
23. Leigh-Smith S, Harris T. Tension pneumothorax—time for a re-think? *Emerg Med J*. 2005; 22:8–16. [PubMed: 15611534]

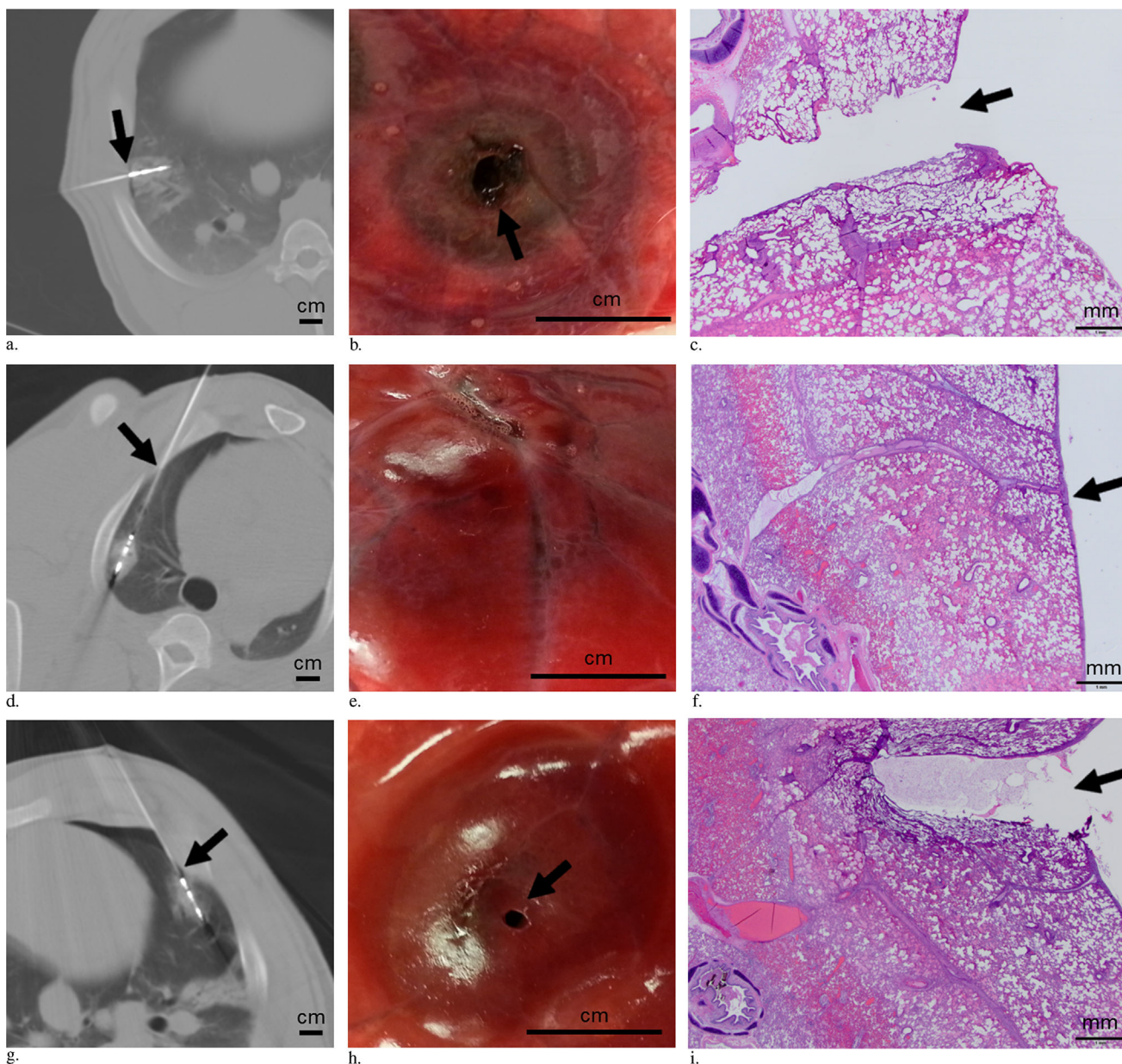


Figure. (a–c) MW ablation performed with the probe in a perpendicular orientation and the ablation zone including the pleural puncture site. (a) CT image shows the probe is perpendicular with respect to the pleura, and the ablation zone includes the pleural puncture site (arrow) (scale bar = 1 cm). (b) Gross specimen shows a hole in the pleura (arrow) with surrounding concentric ring of ablation changes in the lung (scale bar = 1 cm). (c) Photomicrograph of the ablated lung shows disruption of the pleura (arrow) (hematoxylin-eosin [H&E] stain, scale bar = 1 mm). (d–f) MW ablation performed with the probe in a parallel orientation and the ablation zone excluding the pleural puncture site. (d) Axial CT image shows the probe is parallel with respect to the pleura, and the ablation zone does not include the pleural puncture site (arrow) (scale bar = 1 cm). (e) Gross specimen shows intact pleura with

erythema (scale bar = 1 cm). **(f)** Photomicrograph of the ablated lung shows intact pleura (arrow) (H&E stain, scale bar = 1 mm). **(g–i)** MW ablation performed with the probe in a parallel orientation and the ablation zone including the pleural puncture site. **(g)** Axial CT image shows that the probe is parallel with respect to the pleura, and the ablation zone includes the pleural puncture site (arrow) (scale bar = 1 cm). Note the small pneumothorax that developed after the ablation with probe in place. **(h)** Gross specimen shows a hole (arrow) in the pleura with surrounding erythema from ablation change (scale bar = 1 cm). **(i)** Photomicrograph of the ablated lung shows disruption of the pleura (arrow) (H&E stain, scale bar = 1 mm).

Table 1

Swine Demographics and Ablation Characteristics

Variable	Value
Sex	
Female, n	8 (100)
Weight (kg)	40.4 ± 3.1
Ablation power	
30 W	34 (55)
65 W	28 (45)
Ablation time	
5 min	62 (100)
Probe geometry, n	
Parallel	36 (58)
Perpendicular	26 (42)
Lobe, n	
Left lower lobe	19 (31)
Left upper lobe	6 (10)
Right lower lobe	22 (35)
Right middle lobe	7 (11)
Right upper lobe	8 (13)
Emitting point to pleural puncture distance (cm)	2.4 ± 1.2
Emitting point to closest pleura distance (cm)	1.2 ± 0.4
Ablation zone includes pleural puncture site	
Yes	32 (52)
No	30 (48)
Ablation zone long axis (cm)	3.1 ± 0.7
Ablation zone short axis (cm)	2.0 ± 0.5
Ablation zone area (cm ²)	5.0 ± 2.0
Pleural contact with ablation zone (cm)	2.2 ± 1.2

Note—Continuous values were presented as mean ± SD. Values in parentheses are percentages.

Table 2**Pneumothorax after Microwave Ablation**

	No Pneumothorax	Pneumothorax
No.	49 (79)	13 (21)
Ablation power		
30 W	27 (79)	7 (21)
65 W	22 (79)	6 (21)
Temperature (°C)	93 ± 15	91 ± 17
Probe geometry, n		
Perpendicular	18 (69)	8 (31)
Parallel	31 (86)	5 (14)
Probe angle (°)	4 ± 33	966 30
Emitting point to pleural puncture distance (cm)	2.5 ± 1.2	1.9 ± 1.1
Emitting point to closest pleura distance (cm)	1.2 ± 0.5	1.1 ± 0.3
Ablation zone includes pleural puncture site, n		
No	27 (90)	3 (10)
Yes	22 (69)	10 (31)
Ablation zone long axis (cm)	3.2 ± 0.7	3.0 ± 0.7
Ablation zone short axis (cm)	2.0 ± 0.5	1.8 ± 0.4
Ablation zone area (cm ²)	5.2 ± 2.1	4.3 ± 1.6
Pleural contact with ablation zone (cm)	2.2 ± 1.2	2.1 ± 1.0
No. ablations in each lung	2.7 ± 1.5	3.8 ± 1.9
Time since intubation (min)	69 ± 53	122 ± 62

Note—Continuous values were presented at mean ± SD. Values in parentheses are percentages.

Table 3

Univariate Analysis of Factors Predicting Pneumothorax after Microwave Ablation

	Odds Ratio	Confidence Interval	P Value
Ablation power (W)	1.0	0.97–1.04	.94
Temperature (°C)	1.0	0.95–1.03	.66
Probe geometry (perpendicular vs parallel)	2.8	0.78–9.71	.11
Probe angle (°)	1.0	1.00–1.04	.11
Emitting point to pleural puncture distance (cm)	0.6	0.35–1.16	.14
Emitting point to closest pleura distance (cm)	0.5	0.12–2.38	.42
Ablation zone includes pleural puncture site (yes vs no)	4.1	1.00–16.7	.05
Ablation zone long axis (cm)	0.6	0.23–1.64	.33
Ablation zone short axis (cm)	0.4	0.10–1.65	.21
Ablation zone area (cm ²)	0.8	0.55–1.12	.18
Pleural contact with ablation zone (cm)	0.9	0.54–1.55	.74
No. ablations in each lung	1.5	1.03–2.28	.04
Time since intubation (h)	2.8	1.33–5.84	.01

Author Manuscript

Author Manuscript

Author Manuscript

Author Manuscript

Table 4

Multivariate Analysis of Factors Predicting Pneumothorax

	<i>P</i> Value	Odds Ratio	Confidence Interval
Ablation zone includes pleural puncture site (yes vs no)	.02	7.7	1.34–44.5
No. ablations in each lung	.08	1.6	0.95–2.54
Time since intubation (h)	.02	2.7	1.18–6.02

Author Manuscript

Author Manuscript

Author Manuscript

Author Manuscript